Applied Physics Letters

Dual-band MgZnO ultraviolet photodetector integrated with Si

Y. N. Hou, Z. X. Mei, H. L. Liang, D. Q. Ye, C. Z. Gu et al.

Citation: Appl. Phys. Lett. **102**, 153510 (2013); doi: 10.1063/1.4802486
View online: http://dx.doi.org/10.1063/1.4802486
View Table of Contents: http://apl.aip.org/resource/1/APPLAB/v102/i15
Published by the American Institute of Physics.

APPLIED PHYSICS LETTERS **102**, 153510 (2013)

Dual-band MgZnO ultraviolet photodetector integrated with Si

Y. N. Hou, Z. X. Mei,[a)] H. L. Liang, D. Q. Ye, C. Z. Gu, and X. L. Du[a)]
Beijing National Laboratory for Condensed Matter Physics, Institute of Physics, Chinese Academy of Sciences, Beijing 100190, China

(Received 21 January 2013; accepted 5 April 2013; published online 18 April 2013)

We have constructed a dual-band ultraviolet photodetector by growing high quality $Mg_xZn_{1-x}O$ layers on Si substrate with molecular beam epitaxy. The device performance was studied by current-voltage, capacitance-voltage, spectra photoresponse, and time-resolved photoresponse characterizations. It demonstrates a high UV/visible light rejection ratio of more than 2 orders of magnitude and a fast response speed of less than 100 ms. The cutoff wavelength can be at solar-blind (280 nm)/visible-blind (301 nm) region by applying 1 V forward/2 V reverse bias. The working principle of the dual-band photodetector was finally investigated by interpretation of the specific carrier transport behavior with the energy band diagram. © *2013 AIP Publishing LLC*
[http://dx.doi.org/10.1063/1.4802486]

Solid state ultraviolet photodetectors (UV PDs) are very essential in scientific, military, and commercial applications, for example, aerospace UV monitoring, UV imaging, flame detection, missile early warning, and inter-satellite communications.[1,2] Over the last decade, several kinds of wide bandgap semiconductors, such as GaN, SiC, diamond, ZnS, ZnSe, and ZnO, have been developed and applied on UV PDs.[3–5] Among these wide bandgap semiconductors, ZnO with a direct bandgap of 3.37 eV and a large exciton binding energy of 60 meV is recognized as one of the most promising materials for UV PDs.[6,7] By alloying with MgO, it is possible to modulate the band gap of $Mg_xZn_{1-x}O$ from 3.37 to 7.8 eV, which is essential to fabricate UV PDs with different cutoff wavelengths.[8,9] Moreover, modern photoelectric information technology poses urgent need for multi-band UV light detection by using one PD for simultaneous multi-band signal processing.[10] Therefore, high signal to noise (S/N) ratio, high response speed, and cutoff wavelength-selectable UV PDs are strongly desired.[11] However, reports on this type of PDs in the deep UV region are rare. For one thing, it is a big challenge to synthesize high-quality wurtzite $Mg_xZn_{1-x}O$ with the bandgap in deep UV region due to the significant phase segregation problem.[12] Another big issue restricting the practical use of $Mg_xZn_{1-x}O$ UV PDs is the substrate selection. Until now, most of the $Mg_xZn_{1-x}O$ UV PDs have been constructed on insulating sapphire substrates with planar metal-semiconductor-metal (MSM) structures.[13,14] These PDs are not compatible with the mature Si micro-electronic technologies and thus unlikely to be applied in modern integrated circuits. There are some limited reports of $Mg_xZn_{1-x}O$ UV PDs fabricated on Si wafers with cutoff wavelengths in visible-blind region.[15,16]

In our previous work, we have achieved high-Mg content single wurzite phase $Mg_xZn_{1-x}O$ on Si substrates by radio-frequency plasma assisted molecular beam epitaxy (rf-MBE),[17] and UV PDs with different device structures were fabricated and comparatively studied.[18] Based on these achievements, here we report a monolithic dual-band UV PD based on this n-$Mg_xZn_{1-x}O$/p-Si heterostructure which demonstrated a low darkcurrent density with high S/N ratio and fast response speed. By simply switching the polarity of the applied bias voltage, the UV PD's cutoff wavelength can be easily adjusted from the solar-blind region to visible-blind region. From the particular device structure of the PD, the wavelength-selective behavior was well studied.

The PD is configured with a structure of p-Si/BeO/B-MgZnO/L-MgZnO/H-MgZnO as shown in Fig. 1(a), where B-MgZnO stands for thin MgZnO buffer layer with very low Mg content, L-MgZnO the epitaxial layer with moderately low Mg content, and H-MgZnO the epitaxial layer with high Mg content. The 3 nm thin BeO layer is used to serve as a good template for epitaxial growth of MgZnO layers. As the BeO layer has been proven to be an ineffective carrier blocking layer in our previous reports,[17,18] it will be ignored in our following discussions on carrier transportation behavior in this multilayer structure. During the growth, the Mg Knudsen cell is controlled at 362 °C, 383 °C, and 384.5 °C for B-MgZnO, L-MgZnO, and H-MgZnO layers, while keeping the Zn cell and substrate temperature at 310 °C and 450 °C. The in-plane epitaxial relationship is $[11\text{-}20]_{MgZnO}$//$[11\text{-}20]_{BeO}$//$[11\text{-}2]_{Si}$ confirmed by reflection high-energy electron diffraction (RHEED) and transmission electron microscope (TEM).[17] More details of the epitaxial growth can be found elsewhere.[17]

Photoluminescence (PL) and photoluminescence excitation (PLE) spectra were obtained at 13.6 K by using synchrotron radiation source as shown in Figs. 1(b) and 1(c). The four colored curves in Fig. 1(b) are the fitting curves from the PL spectra (black line). It can be seen clearly three of the fitting curves are located at 289 nm (H-MgZnO), 299 nm (L-MgZnO), and 362 nm (B-MgZnO), corresponding to the band edge emissions from three different epitaxial layers. The fitting curve with a peak at 356 nm (red line) is from the L point emission of the Si substrate. To verify our conclusion, a $Mg_{0.5}Zn_{0.5}O$ single layer with similar Mg content to the H-MgZnO layer was fabricated on a sapphire substrate. As shown in the inset of Fig. 1(b), only one prominent emission peak at 291 nm was observed from the PL spectra of $Mg_{0.5}Zn_{0.5}O$/sapphire sample, which is different from the

a)Authors to whom correspondence should be addressed. Electronic addresses: zxmei@aphy.iphy.ac.cn and xldu@aphy.iphy.ac.cn

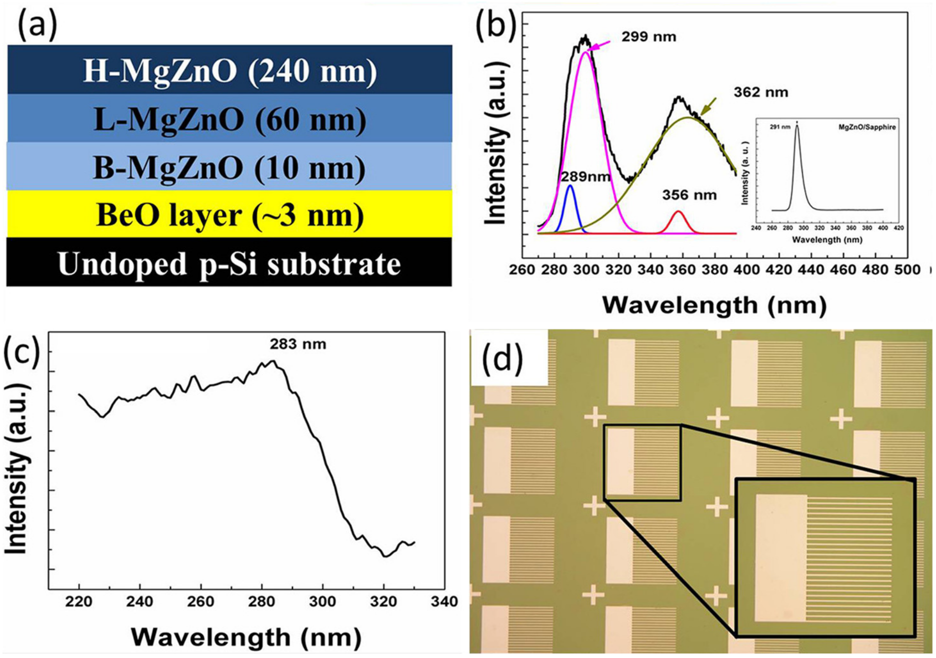

FIG. 1. (a) Structure diagram of the visible blind/solar-blind dual-band UV PD, (b) PL spectrum of the as grown thin films at 13.6 K (black line), the colored lines are fitting curves from the PL (the inset is PL spectrum of $Mg_{0.5}Zn_{0.5}O$/sapphire), (c) PLE spectrum of the thin film at 13.6 K, and (d) top view of the PD in optical microscope.

muti-emission behavior as shown in Fig. 1(b). Comparing Fig. 1(c) with Fig. 1(b), the PLE peak of the H-MgZnO layer is at 283 nm with a 90 meV blue shift from the PL emission. This blue shift is known as Stokes shift which is induced by the inhomogeneous distribution of electrostatic potentials in MgZnO ternary alloys.[19] The PD was finally fabricated by photolithography and liftoff technique with Ti/Au electrode as the front contact on the MgZnO epilayer and indium as the back contact on Si substrate. The top view of the PDs in optical microscope can be seen in Fig. 1(d).

Current-voltage (I-V) measurement result of the PD (Fig. 2(a)) shows a distinct rectifying behavior with a rectification ratio of about 80 under I_{+3V}/I_{-3V}. A low leakage current of 2×10^{-9} A was found at -3 V in the dark, i.e., $1.58 \times 10^{-6}\,\mathrm{A\,cm^{-2}}$, which indicates a good quality of MgZnO/BeO/Si interfaces. In the forward bias, the curve can be divided into two regions as shown in Fig. 2(a). In region I where the applied bias is lower than 2.2 V, the line shape follows the relationship of a p-n junction

$$I = I_0 \exp[(qV/nKT) - 1], \tag{1}$$

where I_0, V, n, K, and T are reverse saturation current, bias voltage, ideality factor, Boltzman constant, and absolute temperature, respectively. By fitting the curve, the value of ideality factor is determined as 8.9. Such a large ideality factor may result from the large series resistance R_s, which is estimated as $4 \times 10^7\,\Omega$ by

$$R_s = dV/dI - nKT/Iq. \tag{2}$$

In region II when the bias rises above 2.2 V, it is not a simple exponential relationship between the current and voltage, which may be caused by the combination of Schottky contact nature of Ti/Au electrode and space charge limited current.[20]

Capacitance-voltage (C-V) measurement was conducted at 10 MHz from -5 V to 4 V. It is found that the capacitance of the PD stays at around 1.49 pF (Fig. 2(b)). We ascribe this to the huge series resistance from MgZnO. Because of the completely depleted thin MgZnO layers (comparing with the thick Si substrate), the depletion depth profile of the device is not seriously changed as almost all the applied bias falls on the MgZnO layers. As a result, the capacitance changes little against applied voltage. Therefore, almost constant capacitance was observed from the C-V measurement. By fitting the curve, the average carrier concentration and the electron mobility of MgZnO film are estimated as $\sim 1 \times 10^{14}\,\mathrm{cm^{-3}}$ and $0.01\,\mathrm{cm\,V^{-1}\,s^{-1}}$, respectively. The strong Mg-O bonding energy in MgZnO alloys results in a large decrease of oxygen vacancy density, which contributes to a significant reduction of n-type carriers. The low carrier mobility is caused by the strong lattice scattering in the deformed MgZnO crystal field. Low mobility always means that the carriers possess low energy; hence, they are prone to being blocked by energy barriers (or band offsets), relating to the device working principle discussed later.

The interesting cutoff wavelength-selectable photoresponse features were shown in Fig. 3(a). When the PD is working under a forward bias of 1 V, we can see that a responsivity of $13\,\mathrm{mA\,W^{-1}}$ with a sharp cutoff at 280 nm corresponds to the optical bandgap of H-MgZnO layer, right in the solar-blind spectrum region. The rejection ratio of solar-blind UV to visible light is about 2 orders of magnitude. While under a reverse 2 V bias, the peak responsivity is $6\,\mathrm{mA\,W^{-1}}$ with a 301 nm cutoff in visible-blind region, corresponding to the optical bandgap of L-MgZnO layer. The shoulder response at 347 nm arises from the thin B-MgZnO layer. Regardless of forward or reverse biases, no visible light response was observed from the silicon substrate.

Response speed is another critical parameter which decides whether a PD can be used in practical applications. In our experiments, transient response was performed by periodic UV illumination. It is found that the PD has a very fast response speed to UV light. The 10%-90% "on" and "off" response time both at forward and reverse biases is less than 100 ms (Fig. 3(b)), which is the limit of our testing system. No persistent photocurrent was observed, indicating a high

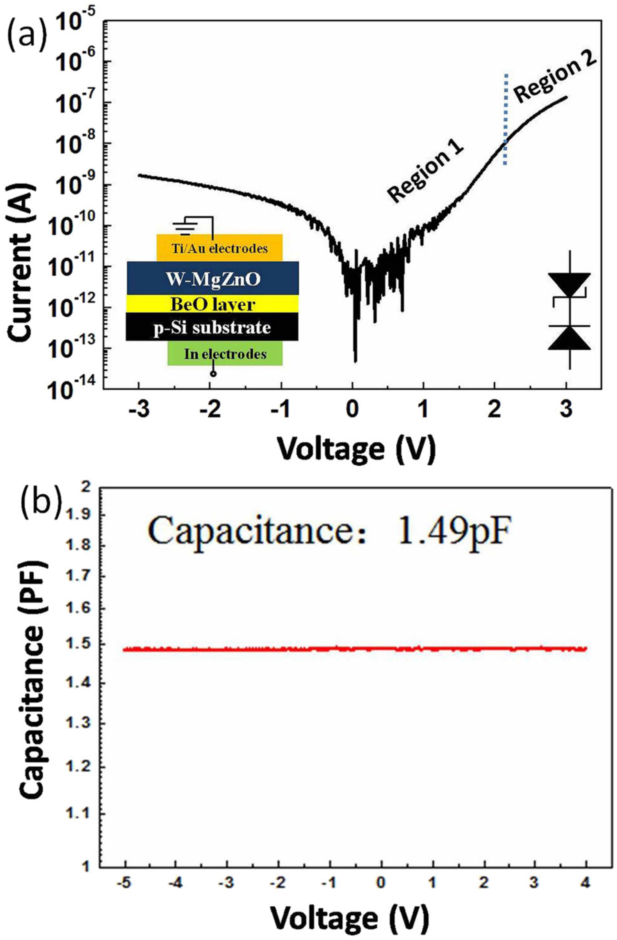

FIG. 2. (a) Dark I-V characteristic of the dual-band UV PD measured from −3 V to 3 V; the insets show the measurement configuration and the equivalent circuit of the PD. (b) C-V measurements of the PD under 10 MHz from −5 V to 4 V.

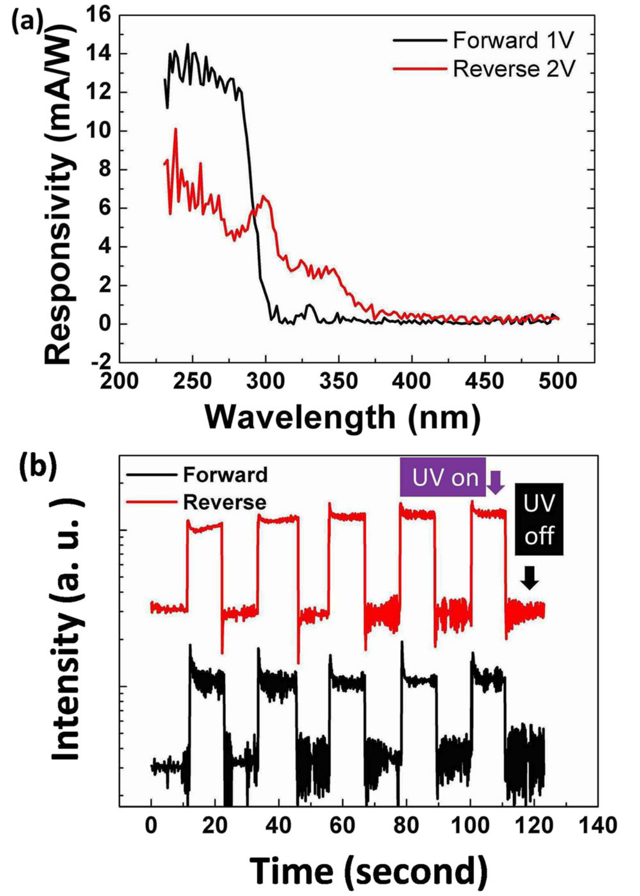

FIG. 3. (a) Photoresponse spectra of the dual-band UV PD at forward and reverse biases. (b) Transient response of the dual-band UV PD.

crystalline quality of the film with very few deep level defects or interface states.[21,22]

To understand the working principle of the solar-blind/visible-blind selective UV PD, we used the energy band diagram which was schematically drawn according to Anderson-Shockley model. As shown in Fig. 4(a) under equilibrium condition, type-II heterojunction forms at the B-MgZnO/Si interface whilst type-I heterojunctions form between the three MgZnO epitaxial layers. When the UV PD is under illumination at a forward bias as shown in Fig. 4(b), photons with energy higher than 4.4 eV (wavelength <280 nm) will be strongly absorbed near the surface of the H-MgZnO layer and hence generate electron-hole (e-h) pairs. Under the driving force of the electrical field, the photon-generated holes and electrons can easily drift to the Ti/Au electrodes and Si substrate, respectively, raising a strong solar-blind response at 280 nm (black line in Fig. 3(a)). In the case of lower energy (wavelength >280 nm) illumination, photons can penetrate the H-MgZnO layer and be absorbed by low-Mg content L-MgZnO, B-MgZnO, and Si. However, the photon-generated holes will be effectively blocked by the barriers of valence band offsets and recombine with the electrons, making no contribution to electrical conduction. Therefore, only solar-blind photoresponse from the H-MgZnO layer was observed at forward bias.

However, when the PD is under illumination at a reverse bias, as shown in Fig. 4(c), the situation is much different. Because of the limit penetration depth of UV rays in wide bandgap semiconductors (around 50 nm for MgZnO),[23] photon-generated e-h pairs by UV light will congregate near the surface of H-MgZnO layer in the case of illumination with a wavelength less than 280 nm. Holes cannot immediately transport through the whole H-MgZnO layer to reach Si substrate due to its low mobility as mentioned above but

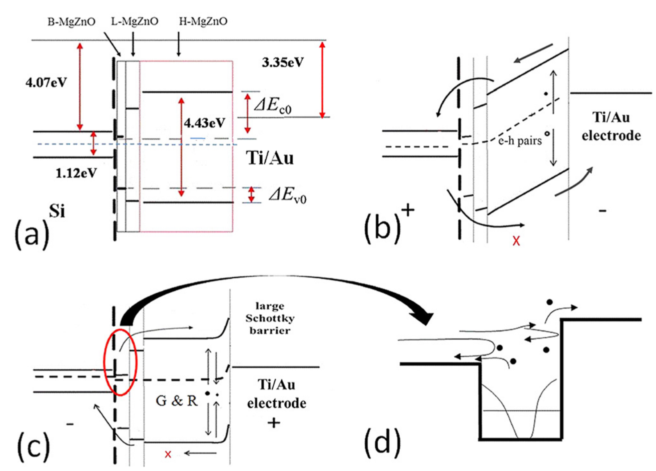

FIG. 4. Energy-band diagram of the UV PD (a) under equilibrium condition, (b) under illumination at forward bias, (c) under illumination at reverse bias, and (d) schematic of electron-electron scattering process in an asymmetric quantum well.

rapidly recombine with those electrons which are blocked by the Schottky barrier before forming a distinct photocurrent. The L-MgZnO layer is much thinner and closer to the Si substrate. Therefore holes generated by lower energy photons can transport to the Si substrate easily, resulting a UV-B response at a wavelength of 301 nm (red line in Fig. 3(a)). The shoulder response at 347 nm from the B-MgZnO layer was observed in a similar fashion. Interestingly there is no visible light response from Si substrate at reverse bias either, which can be illustrated by the electron-electron scattering process in an asymmetric quantum well.[24] Notice the conduction band minimum of B-MgZnO layer falls between those of the Si substrate and L-MgZnO layer, forming an asymmetric electron well as shown in Fig. 4(d). Photon-generated electrons in Si were scattered by electrons from this quantum well and the barrier at B-MgZnO/L-MgZnO interface. As a consequence, the electrons generated in Si wafer by visible light illumination cannot reach the H-MgZnO side to form photocurrent. Additionally, due to a series of band offsets for electrons, the responsivity at reverse bias is much lower than that at forward bias as shown in Fig. 3(a). Although the value of photoresponsivity at both forward and reverse biases is still not high enough, we believe it can be promoted by further optimization of the device structures.

In summary, a type of cutoff wavelength-selectable UV PD was invented by growing high-quality wurzite $Mg_xZn_{1-x}O$ layers with different Mg contents on Si substrate using rf-MBE technique. By simply controlling the polarity of the applied bias, the PD can respond to either solar-blind waveband or visible-blind waveband with sharp cutoff wavelengths. The UV/visible rejection ratio is about 2 orders of magnitude with a fast response speed less than 100 ms. This kind of PD combines the important 3rd-generation oxide semiconductor with the well-developed 1st-generation Si semiconductor, which we believe will have a strong influence on the realization of integrated multi-band UV detectors.

This work was supported by the Ministry of Science and Technology (Grant Nos. 2011CB302002, 2011CB302006, and 2009CB929404) of China, the National Science Foundation (Grant Nos. 61076007, 11174348, 51272280, 11274366, and 61204067), Chinese Academy of Sciences, and Beijing Synchrotron Radiation Facility.

[1]H. W. Lin, S. Y. Ku, H. C. Su, C. W. Huang, Y. T. Lin, K. T. Wong, and C. C. Wu, Adv. Mater. **17**, 2489 (2005).
[2]W. Yang, R. D. Vispute, S. Choopun, R. P. Sharma, T. Venkatesan, and H. Shen, Appl. Phys. Lett. **78**, 2787 (2001).
[3]M. Razeghi and A. Rogalski, J. Appl. Phys. **79**, 7433 (1996).
[4]K. Liu, M. Sakurai, and M. Aono, Sensors **10**, 8604 (2010).
[5]A. Sciuto, F. Roccaforte, S. Di Franco, V. Raineri, S. Billotta, and G. Bonanno, Appl. Phys. Lett. **90**, 223507 (2007).
[6]D. C. Look, Mater. Sci. Eng. B **80**, 383 (2001).
[7]H. Tanaka, S. Fujita, and S. Fujita, Appl. Phys. Lett. **86**, 192911 (2005).
[8]A. Schleife, M. Eisenacher, C. Rödl, F. Fuchs, J. Furthemüller, and F. Bechestedt, Phys. Rev. B **81**, 245210 (2010).
[9]X. H. Xie, Z. Z. Zhang, C. X. Shan, H. Y. Chen, and D. Z. Shen, Appl. Phys. Lett. **101**, 081104 (2012).
[10]L. C. Lenchyshyn, H. C. Liu, M. Buchanan, and Z. R. Wasilewski, J. Appl. Phys. **79**, 8091 (1996).
[11]Y. Hu, J. Zhou, P. H. Yeh, Z. Li, T. Y. Wei, and Z. L. Wang, Adv. Mater. **22**, 3327 (2010).
[12]X. L. Du, Z. X. Mei, Z. L. Liu, Y. Guo, T. C. Zhang, Y. N. Hou, Z. Zhang, Q. K. Xue, and A. Y. Kuznetsov, Adv. Mater. **21**, 4625 (2009).
[13]Y. N. Hou, Z. X. Mei, Z. L. Liu, T. C. Zhang, and X. L. Du, Appl. Phys. Lett. **98**, 103506 (2011).
[14]C. Z. Wu, L. W. Ji, C. H. Liu, S. M. Peng, S. J. Yong, K. T. Lam, and C. J. Huang, J. Vac. Sci. Technol. A **29**, 03A118 (2011).
[15]M. Fujita, M. Sasajima, Y. Deesirapipat, and Y. Horikoshi, J. Cryst. Growth **278**, 293 (2005).
[16]K. Koike, K. Hama, I. Nakashima, G. Y. Takada, K. I. Ogata, S. Sasa, M. Inoue, and M. Yano, J. Cryst. Growth **278**, 288 (2005).
[17]H. L. Liang, Z. X. Mei, Q. H. Zhang, L. Gu, S. Liang, Y. N. Hou, D. Q. Ye, C. Z. Gu, R. C. Yu, and X. L. Du, Appl. Phys. Lett. **98**, 221902 (2011).
[18]Y. N. Hou, Z. X. Mei, H. L. Liang, D. Q. Ye, S. Liang, C. Z. Gu, and X. L. Du, Appl. Phys. Lett. **98**, 263501 (2011).
[19]Z. L. Liu, Z. X. Mei, R. Wang, J. M. Zhao, H. L. Liang, Y. Guo, A. Yu. Kuznetsov, and X. L. Du, J. Phys. D: Appl. Phys. **43**, 285402 (2010).
[20]Ş. Aydoğan, K. Çınar, H. Asıl, C. Coşkun, and A. Türüt, J. Alloys Compd. **476**, 913 (2009).
[21]C. V. Reddy, K. Balakrishnan, H. Okumura, and S. Yoshida, Appl. Phys. Lett. **73**, 244 (1998).
[22]O. Katz, G. Bahir, and J. Salzman, Appl. Phys. Lett. **84**, 4092 (2004).
[23]M. Nakano, T. Makino, A. Tsukazaki, K. Ueno, A. Ohtomo, T. Fukumura, H. Yuji, S. Akasaka, K. Tamura, K. Nakahara, T. Tanabe, A. Kamisawa, and M. Kawasaki, Appl. Phys. Lett. **93**, 123309 (2008).
[24]P. Kinsler, P. Harrison, and R. W. Kelsall, Phys. Rev. B **58**, 4771 (1998).